

# A Novel Prediction-based Spectrum Allocation Mechanism for Mobile Cognitive Radio Networks

Yao Wang<sup>1,2,3</sup>, Zhongzhao Zhang<sup>1</sup>, Qiyue Yu<sup>1</sup> and Jiamei Chen<sup>1</sup>

<sup>1</sup>Communication Research Center, Harbin Institute of Technology  
Harbin, 150080 - China  
[e-mail: wangyaowh2005@126.com]

<sup>2</sup>Communication Department, Shenyang Artillery Academy  
Shenyang, 110867 – China

<sup>3</sup>Science and Technology on Information Transmission and Dissemination in Communication Networks  
Laboratory  
Shijiazhuang, 050081 – China

\*Corresponding author: Yao Wang

*Received May 27, 2013; revised July 31, 2013; accepted September 8, 2013; published September 30, 2013*

---

## Abstract

The spectrum allocation is an attractive issue for mobile cognitive radio (CR) network. However, the time-varying characteristic of the spectrum allocation is not fully investigated. Thus, this paper originally deduces the probabilities of spectrum availability and interference constrain in theory under the mobile environment. Then, we propose a prediction mechanism of the time-varying available spectrum lists and the dynamic interference topologies. By considering the node mobility and primary users' (PUs') activity, the mechanism is capable of overcoming the static shortcomings of traditional model. Based on the mechanism, two prediction-based spectrum allocation algorithms, prediction greedy algorithm (PGA) and prediction fairness algorithm (PFA), are presented to enhance the spectrum utilization and improve the fairness. Moreover, new utility functions are redefined to measure the effectiveness of different schemes in the mobile CR network. Simulation results show that PGA gets more average effective spectrums than the traditional schemes, when the mean idle time of PUs is high. And PFA could achieve good system fairness performance, especially when the speeds of cognitive nodes are high.

---

**Keywords:** Cognitive radio, spectrum allocation, prediction, mobility, graph theory, PUs' activity

---

This research was supported by National Natural Science Foundation and Civil Aviation Administration of China (Grant No. 61101122 and 61071104) and Science and Technology on Information Transmission and Dissemination in Communication Networks Laboratory (Grant No. ITD-U12004/K1260010).

<http://dx.doi.org/10.3837/tiis.2013.09.002>

## 1. Introduction

Cognitive radio (CR) is considered as a feasible intelligent technology for 4G wireless networks or self-organization networks [1][2]. Secondary users (SUs) can opportunistically access the licensed spectrum without causing interferences to the PUs [3]. Thus, it is necessary to have an optimal MAC layer schedule. Graph coloring model, as a tool for spectrum allocation, has been widely investigated these days [4][5]. The optimal coloring problem of a graph is known to be NP-hard. Thus, recent works focus on heuristic approaches to close to the optimal spectrum allocation solutions. Ref. [6] presented greedy algorithm (GA) achieving close to optimal spectrum utilization and fairness algorithm (FA) getting better allocation fairness. Peng and Zheng first considered color sensitive graph coloring (CSGC) algorithm for the heterogeneity in the spectrum rewards in Ref. [7], in which a graph-theoretical model was developed to characterize the spectrum access problem under a number of different functions of optimizing utilization and fairness. To reduce the allocation duration of CSGC, paper [8] presented a kind of parallel algorithm that divided bidirectional graph in CSGC into many simple subgraphs; however the parallel algorithm cannot work under constraint of fairness rules. While, a maximal independent set (MIS) spectrum allocation algorithm based on graph theory was presented with the goal of enhancing fairness [9].

However, most of the existing graph-based spectrum allocation schemes for the CR network are based on the network snapshot model, which means these schemes focus on a static spectrum environment. Actually, the static spectrum allocation is based on the assumptions that both the PUs and the SUs are fixed during simulations, however, this assumption is impractical for a mobile situation.

In practice, the spectrum availability is time-varying due to the random variations of the arrivals and departures of PUs. Therefore, some works have focused on the impact of PUs' on-off behaviors [10][11][12]. In [13], a continuous-time Markov chain model was proposed to model the interactions between PUs and SUs. Paper [14] presented a prediction approach for call arrival rate and call holding time of PUs. By the traffic pattern forecast of PUs, SUs can estimate the utilization of frequency bands, thus reduces the frequency hopping rate. The spectrum prediction is more effective for throughput optimization by a new definition of channel availability vector that characterized the licensed channels state information [15].

On the other hand, mobility is an important factor in mobile wireless communications [16]. However, the mobility of nodes is not fully investigated for spectrum allocation in CR network. In [17], a cluster-based spectrum and interference aware routing protocol is proposed to repair the route considering PUs' activity for mobile CR networks. Moreover, the routing protocol can increase throughput and reduce data delivery latency. The author proposed a topology control and routing scheme to improve end-to-end network performance, i.e., throughput and delay [18].

In fact, a reactive CR system without prediction will degrade system performance because spectrum sensing may be delayed or take a long time [19][20]. Thus, a CR network should be forward looking rather than reactive [21]. In this paper, we focus on prediction spectrum allocation mechanism in mobile cognitive radio networks. Our main contributions can be summarized as follows: 1) we extend the traditional static graph-based model [4][5][6][7][8][9] to dynamic mobile model. Based on deducing the probabilities of spectrum availability and interference constrain in theory under the mobile model, a prediction mechanism considering node mobility and PUs' states is presented. 2) Two novel prediction-based spectrum assignment algorithms (PGA and PFA) aiming at maximizing spectrum utilization and

fairness are respectively proposed on the basis of the predictions mechanism. 3) New utility functions which investigate spectrum utilization and fairness are redefined in order to evaluate the performance of different algorithms under the mobile CR environment. 4) Finally, we conduct some simulations to confirm the accuracy of the prediction mechanism and the utilities of the prediction-based spectrum allocation algorithms. Compared with the conventional GA and FA, the proposed schemes achieve high spectrum utilization and fairness utilities respectively when the prediction performance is accurate relatively.

The rest of the paper is organized as follows. The system model is described in Section 2, and the predictions of spectrum availability and interference constraints for cognitive nodes are discussed in Section 3. In Section 4, two novel prediction-based spectrum allocation algorithms are proposed. We will show the simulation results along with a discussion in Section 5. And Section 6 concludes the paper.

## 2. System Model and Utility Function

### 2.1 System Model

Consider a mobile CR network deployment scenario where  $N$  SUs coexist with  $M$  PUs depicted in **Fig. 1**. Each primary user (PU) is composed of a primary base station (PBS) and a group of primary receivers. Suppose each PU has a coverage area, and PBS determines the PU's coverage area. In the model, PU is allowed to use the associated licensed channel, while SUs can use the licensed channels opportunistically. In other words, SUs within the coverage area of one PU are not allowed to use the corresponding licensed channel when the PU is active. Additionally, we assume that CR network assigns spectrums periodically, and the spectrum allocation duration is very short which can be neglected. And set the spectrum allocation time interval is  $T_c$ . The activity of each PU is modeled as an active/inactive (on/off) scheme independently. The time intervals of the active and inactive states follow exponential distributions with means  $1/\lambda_p$  and  $1/\mu_p$ , respectively [22][23][24]. So the active and inactive probability density function can be written respectively as

$$f_{\text{ON}}(t) = \begin{cases} \lambda_p e^{-\lambda_p t} & t \geq 0 \\ 0 & t < 0 \end{cases} \quad (1)$$

$$f_{\text{OFF}}(t) = \begin{cases} \mu_p e^{-\mu_p t} & t \geq 0 \\ 0 & t < 0 \end{cases} \quad (2)$$

A random walk-based mobility model is proposed in paper [25]. Suppose mobility of cognitive nodes is uncorrelated, and each node's movement consists of a sequence of random length intervals called mobility epochs, during which a node moves in a constant direction at a constant speed. Therefore, the mobility of a given node  $n$  is based on epoch lengths, speed, and direction. Epoch lengths are exponentially distributed with mean  $1/\lambda$  [25][26], denoted as

$$B(x) = P(T \leq x) = 1 - e^{-\lambda x} \quad (3)$$

The speed of node  $n$  is a uniform distributed over  $(0, v_{\text{max}})$  and the direction is an IID uniformly distributed over  $(0, 2\pi)$ . It is reasonable to assume the speed, direction and epoch lengths of node  $n$  are uncorrelated. **Fig. 1** is an instantaneous snapshot of a CR network, in which 20 mobile cognitive nodes are uniform distributed in the deployment area. The movement characteristics (speed, direction and epoch lengths) of any two different nodes are also uncorrelated. And the interference radius of each cognitive node is  $r$ . In the mobile CR

network deployment area, 2 PUs (PU1 and PU2) are located. The coverage radius of each PU is  $R$ .

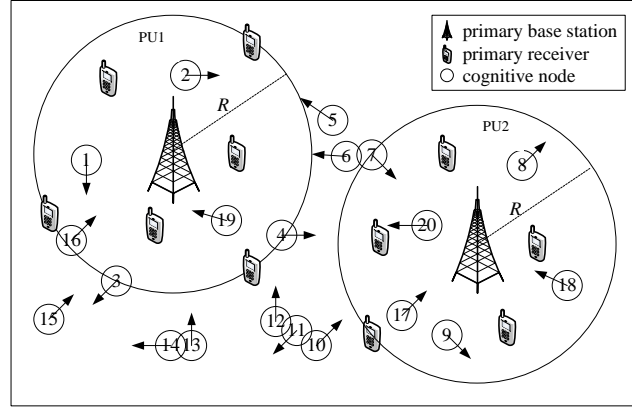


**Fig. 1.** System model of cognitive network

Based on the proposed mobile model, two kinds of issues need to be investigated. One is the available spectrum lists of the cognitive nodes. The other is the interference constrains of the cognitive nodes. First, each cognitive node has an available spectrum list, and it is obvious that the available spectrum list is time-varying due to the mobility of the cognitive nodes and the changing activities of PUs. So, one cognitive node  $n$  can use the licensed channel  $m$  at  $t$  only if  $l_{m,n}(t)=1$  with  $l_{m,n}(t)$  given as

$$l_{m,n}(t) = \begin{cases} 1 & D_{\text{PU}_m, \text{SU}_n}(t) \geq R + r \\ 1 & D_{\text{PU}_m, \text{SU}_n}(t) < R + r \cap (\alpha_m(t) = 1) \\ 0 & D_{\text{PU}_m, \text{SU}_n}(t) < R + r \cap (\alpha_m(t) = 0) \end{cases}, \quad (4)$$

where  $D_{\text{PU}_m, \text{SU}_n}(t)$  is the distance between  $\text{PU}_m$  and cognitive node  $n$  at  $t$ , and  $\alpha_m(t)$  represents the activity state of  $\text{PU}_m$ , given as

$$\alpha_m(t) = \begin{cases} 1 & \text{PU}_m \text{ is idle at } t \\ 0 & \text{PU}_m \text{ is busy at } t \end{cases}. \quad (5)$$

In practice,  $l_{m,n}(t)$  is mainly depended on the position of node  $n$  and the state of  $\text{PU}_m$ . (4) reflects the instantaneous spectrum availability.  $l_{m,n}(t)=1$  denotes licensed spectrum  $m$  is available to cognitive node  $n$  at  $t$ .  $l_{m,n}(t)=0$  denotes licensed spectrum  $m$  is not available to cognitive node  $n$  at  $t$ . Next, we need to state interference constrain. Instantaneous interference constrain  $e_{i,j}(t)$  for any two different cognitive nodes  $i$  and  $j$  at  $t$  can be expressed as

$$e_{i,j}(t) = \begin{cases} 1 & D_{\text{SU}_i, \text{SU}_j}(t) < 2r \cap (i \neq j) \\ 0 & D_{\text{SU}_i, \text{SU}_j}(t) \geq 2r \cap (i \neq j) \end{cases}. \quad (6)$$

$D_{\text{SU}_i, \text{SU}_j}(t)$  is the distance between node  $i$  and node  $j$  at  $t$ .  $e_{i,j}(t)=1$  represents that node  $i$  and node  $j$  have interference constrain if they use the same licensed spectrum at  $t$ .  $e_{i,j}(t)=0$  represents that node  $i$  and node  $j$  don't have interference constrain if they use the same licensed spectrum at  $t$ . Therefore, interference constrain reflects that any two different cognitive nodes will impact each other if they use the same licensed channel simultaneously. Note that both available spectrum lists and interference constrains mentioned above are instantaneous.

## 2.2 Utility Functions

In order to measure the accuracy of the proposed prediction mechanism, two evaluation parameters are given first. Available spectrum prediction error rate  $\rho_s$  is given as

$$\rho_s = \frac{\sum_{n=1}^N (M_n^{\text{alarm}} + M_n^{\text{dismissal}})}{\sum_{n=1}^N M_n^{\text{total}}}, \quad (7)$$

where  $M_n^{\text{total}}$  is the total number of available spectrums for node  $n$ .  $M_n^{\text{dismissal}}$  is the total number of spectrums for node  $n$  which are not counted by the prediction mechanism while these spectrums should be included in the real available spectrum set.  $M_n^{\text{alarm}}$  is the total number of spectrums for node  $n$  which are counted by the prediction mechanism while these spectrums should not be included in the real available spectrum set. Actually,  $M_n^{\text{dismissal}}$  represents the number of available spectrums for false dismissal and  $M_n^{\text{alarm}}$  represents the number of available spectrums for false alarm. The bigger  $\rho_s$  is, the worse the accuracy of available spectrum prediction mechanism is. Similar to the definition of  $\rho_s$ , interference constrain prediction error rate  $\rho_l$  is given as

$$\rho_l = \frac{N_{\text{alarm}} + N_{\text{dismissal}}}{N_{\text{total}}}, \quad (8)$$

where  $N_{\text{total}}$  is the total number of interference constrains for the mobile CR network.  $N_{\text{alarm}}$  represents the number of interference constrains for false alarm. And  $N_{\text{dismissal}}$  represents the number of interference constrains for false dismissal.

In addition, we need to redefine the utility functions of spectrum allocation owing to the mobile CR model. Traditionally, the objective of the spectrum allocation problem can be defined as utility functions [27]:

Max-Sum-Bandwidth (MSB): it aims to maximize the total spectrum utilization regardless of fairness for the CR network. The utility function is defined as

$$U_{\text{sum}} = \frac{1}{N} \sum_{n=1}^N \sum_{m=1}^M a_{n,m} \cdot b_{n,m}, \quad (9)$$

where  $a_{n,m}=1$  represents that spectrum  $m$  is assigned to node  $n$ , and  $b_{n,m}$  means the reward that node  $n$  can get if spectrum  $m$  is assigned to node  $n$ .

Max-Proportional-Fair (MPF): it focuses on the proportional fairness for the CR network. The utility function is expressed as

$$U_{\text{fair}} = \sum_{n=1}^N \lg \left( \sum_{m=1}^M a_{n,m} \cdot b_{n,m} \right). \quad (10)$$

MSB rule is relatively selfish and non-collaborative, while MPF rule characterizes fairness and collaboration. Owing to the mobile CR model, the utility function  $U_{\text{sum}}$  is redefined as

$$U_1 = \frac{1}{N} \sum_{n=1}^N \sum_{m=1}^M a_{n,m} \cdot b_{n,m} \quad (n,m) \in S, \quad (11)$$

where  $(n,m) \in S$  denotes the licensed spectrum  $m$  is available to cognitive node  $n$  from  $t_0$  to  $t_0+T_c$ . It means that spectrum  $m$  is available to cognitive node  $n$  not only at  $t_0$  but also at any time between  $t_0$  and  $t_0+T_c$ .

$$S = \{(n,m) | l_{n,m}(t) = 1 \text{ from } t_0 \text{ to } t_0 + T_c\}. \quad (12)$$

In fact,  $U_1$  reflects the ‘effective’ spectrums one cognitive node can get during  $T_c$  on average. Nevertheless,  $U_1$  cannot measure the fairness among different nodes.  $U_{\text{fair}}$  is redefined as

$$U_2 = \frac{1}{N} \sum_{n=1}^N \lg \left( \sum_{m=1}^M a_{n,m} \cdot b_{n,m} + \Delta \right) \quad (n,m) \in S. \quad (13)$$

$\Delta$  ( $0 < \Delta \ll 1$ ) is very small positive number to prevent the antilogarithm from being equal to zero.  $U_2$  reflects the difference of ‘effective’ spectrums that different cognitive nodes can get during  $T_c$ . The bigger  $U_2$  is, the higher the CR network fairness performance is.  $U_1$  and  $U_2$  are defined to reflect time-varying features.

### 3. Prediction of Spectrum Availability and Interference Constrains

Actually, spectrum availability and interference constrain varies with the time  $t$  due to the mobility of the CR networks. This paper mainly considers the continuous states of spectrum availability and interference constrain for a period such as  $T_c$ , and then presents prediction spectrum allocation schemes. First, the probabilities of spectrum availability and interference constrain will be deduced under the mobile CR model in the following sub-sections.

#### 3.1 Prediction of Spectrum Availability for Cognitive Nodes

The spectrum availability of one cognitive node varies because of the node’s mobility and PUs’ arrivals/departures with the time  $t$ . Thus, the spectrum availability prediction of one cognitive node includes two parts. One is the prediction of busy/idle activities for PUs. The other is the prediction of relative positions between PUs and cognitive nodes. Moreover, it is obvious that the two parts need to be considered together. First, we state spectrum availability which is different from (4), denoted by  $A_n^m(T)$

$$A_n^m(T) = \{\text{The availability of spectrum } m \text{ for cognitive node } n \text{ lasts from } t_0 \text{ to } t_0 + T\}. \quad (14)$$

$A_n^m(T)$  means that spectrum  $m$  is available to cognitive node  $n$  for a continuous time period  $T$ . It is noted that we focus only on two kinds of the cognitive nodes based on the mobile model. The first kind is the nodes which are not in the coverage area of  $\text{PU}_m$  at  $t_0$ . The second kind is the nodes which are in the coverage area of  $\text{PU}_m$  while  $\text{PU}_m$  is idle at  $t_0$ . In other words, it is not necessary to predict the spectrum availability of one node if the node is in the interference region of a busy  $\text{PU}_m$  at  $t_0$ . It is because the spectrum availability can be directly detected by spectrum sensing.

First, we investigate the situation that cognitive node  $n$  is not in the coverage area of  $\text{PU}_m$  at  $t_0$ . The main idea is to let node  $n$  predict a continuous time period  $T_p$  that spectrum  $m$  being available to node  $n$  will last its availability during  $T_p$ . Our goal is to get spectrum availability  $A_n^m(T_c)$  during  $T_c$  by calculating  $A_n^m(T_p)$ . In practice,  $A_n^m(T_p)$  mainly includes two parts:  $A_1(T_p)$  and  $A_2(T_p)$ .  $A_1(T_p)$  indicates the probability that node  $n$  does not move into the coverage area of  $\text{PU}_m$  from  $t_0$  to  $t_0 + T_p$ .  $A_2(T_p)$  indicates the probability that node  $n$  moves into the coverage area of  $\text{PU}_m$  at  $t_0 + T_x$  ( $0 \leq T_x \leq T_p$ ) while  $\text{PU}_m$  is idle from  $t_0 + T_x$  to  $t_0 + T_p$ . Actually,  $A_n^m(T_p)$  also contains other complicated situations.

However,  $A_1(T_p)$  and  $A_2(T_p)$  dominate the main parts considering the short allocation interval time. The calculation of  $A_1(T_p)$  also consists of two parts:  $P_{out1}$  and  $P_{out2}$ .

$$A_1(T_p) = P_{out1} + P_{out2}, \quad (15)$$

where  $P_{out1}$  represents the situation that the velocity of the node  $n$  remains unchanged between  $t_0$  to  $t_0 + T_p$  and  $P_{out2}$  represents the other situations. According to (3),  $P_{out1}$  is easy to get as

$$P_{out1} = 1 - B(T_p) = e^{-\lambda T_p}. \quad (16)$$

However, the accurate calculation of  $P_{out2}$  is complicated because it is difficult to know the spectrum availability caused by the changes of velocity for node  $n$ . Next, we try to get the approximate value  $E(P_{out2})$  by estimating  $P_{out2}$ . Denote a random variable  $\Phi < T_p$  for a time interval between  $t_0$  and  $t_0 + T_p$  during which node  $n$  changes its velocity. Then,  $P(\phi \leq \Phi < T_p)$  indicates the probability that node  $n$  keeps its velocity unchanged from  $t_0$  to  $t_0 + \phi$  while node  $n$  changes its velocity after  $t_0 + \phi$ . And  $P(\phi \leq \Phi < T_p)$  is easy to get as

$$P(\phi \leq \Phi < T_p) = B(T_p) - B(\phi) = (1 - e^{-\lambda T_p}) - (1 - e^{-\lambda \phi}) = e^{-\lambda \phi} - e^{-\lambda T_p}. \quad (17)$$

The approximate value  $E(P_{out2})$  is defined as

$$E(P_{out2}) = \int_0^{T_p} l_2(\phi) f(\phi) d\phi, \quad (18)$$

where  $l_2(\phi)$  is a function of  $\phi$ . In order to get  $l_2(\phi)$ , we first calculate the continuous total time  $T_i$  that node  $n$  will not move into the coverage area of  $PU_m$  if velocity changes happen between  $t_0$  to  $t_0 + T_p$ . After the first change happens at  $t_0 + \phi$ , node  $n$  still has a great probability of staying out of the coverage area of  $PU_m$ . And the probability of the velocity keeping unchanged for node  $n$  from  $t_0 + \phi$  to  $t_0 + T_p$  is  $e^{-\lambda(T_p - \phi)}$  by (3). Thus, the total time  $T_i$  that node  $n$  will not move into the coverage area of  $PU_m$  can be written as

$$T_i = \phi + (T_p - \phi) p_a e^{-\lambda(T_p - \phi)} + \varepsilon_a, \quad (19)$$

where  $p_a$  is the probability for node  $n$  moving far away from  $PU_m$  after the first velocity change.  $\varepsilon_a \geq 0$  is used to include all the situations that are not calculated by  $\phi + (T_p - \phi) p_a e^{-\lambda(T_p - \phi)}$ . Therefore, we can get  $l_2(\phi)$  as

$$l_2(\phi) = \frac{\phi + (T_p - \phi) p_a e^{-\lambda(T_p - \phi)}}{T_p} + \varepsilon_a, \quad (20)$$

$f(\phi)$  is given by

$$f(\phi) = \lim_{\Delta\phi \rightarrow 0} \frac{P(\phi \leq \Phi < T_p) - P(\phi + \Delta\phi \leq \Phi < T_p)}{\Delta\phi} = \lambda e^{-\lambda \phi}. \quad (21)$$

When  $T_p < T_c$  is satisfied, node  $n$  should change its velocity (speed or direction) before  $t_0 + T_p$ , which makes node  $n$  moving far away from  $PU_m$ . According to (18), (20), and (21), the spectrum availability  $A_n^m(T_c)$  for node  $n$  is derived as

$$A_n^m(T_c) \approx E(P_{out2}) = \frac{1}{\lambda T_p} + \varepsilon_a + e^{-\lambda T_p} \left( \frac{1}{2} p_a \lambda T_p - \frac{1}{\lambda T_p} - \varepsilon_a - 1 \right). \quad (22)$$

When  $T_p \geq T_c$  is satisfied, the spectrum availability  $A_n^m(T_c)$  for node  $n$  is derived as

$$A_n^m(T_c) \approx A_1(T_c) + E(P_{\text{out}2}) = \frac{1}{\lambda T_c} + \varepsilon_a + e^{-\lambda T_c} \left( \frac{1}{2} p_a \lambda T_c - \frac{1}{\lambda T_c} - \varepsilon_a \right). \quad (23)$$

It is noted that  $\varepsilon_a$  includes other situations which could happen as small probability events. For instance, node  $n$  changes its velocity for more than two times, which makes node  $n$  still not moves into the coverage area of  $\text{PU}_m$  during  $T_c$ .

Next, we investigate the situation that cognitive node  $n$  is in the coverage area of  $\text{PU}_m$  while  $\text{PU}_m$  is inactive at  $t_0$ . We need to investigate not only the movement of node  $n$  but also the duration of the idle state for  $\text{PU}_m$  from  $t_0$ . Furthermore, we believe that the prediction of the idle state for  $\text{PU}_m$  is more important unlike the first situation, which is because of the initial position of node  $n$ . Similar to the analysis method of the first situation mentioned above, the main idea is to let node  $n$  predict a continuous time period  $T_p^{\text{out}}$  that node  $n$  will not move out of the coverage area of  $\text{PU}_m$  during  $T_p^{\text{out}}$ . Note that  $T_p^{\text{out}}$  is different from  $T_p$ .

When  $T_p^{\text{out}} < T_c$  is satisfied,  $A_n^m(T_c)$  for node  $n$  is derived as

$$A_n^m(T_c) = P_{\text{in}} \cdot \int_{t_0}^{t_0 + T_p^{\text{out}}} f_{\text{OFF}}(t) dt + \varepsilon_{\text{in}}, \quad (24)$$

where  $\int_{t_0}^{t_0 + T_p^{\text{out}}} f_{\text{OFF}}(t) dt$  denotes the idle probability of spectrum  $m$  from  $t_0$  to  $t_0 + T_p^{\text{out}}$ .  $\varepsilon_{\text{in}}$  tries to include all the other spectrum availability situations.  $P_{\text{in}}$  denotes the probability that node  $n$  moves out of the coverage area of  $\text{PU}_m$  before  $t_0 + T_p^{\text{out}}$ .  $P_{\text{in}}$  also includes two parts.  $P_{\text{in}1}$  represents the situation that the velocity of the node  $n$  remains unchanged between  $t_0$  to  $t_0 + T_p^{\text{out}}$ .  $P_{\text{in}2}$  represents the other situations.  $P_{\text{in}}$  can be written as

$$P_{\text{in}} = \frac{1}{\lambda T_p^{\text{out}}} + \varepsilon_b + e^{-\lambda T_p} \left( \frac{1}{2} p_b \lambda T_p^{\text{out}} - \frac{1}{\lambda T_p^{\text{out}}} - \varepsilon_b \right), \quad (25)$$

where  $p_b$  denotes the probability for node  $n$  moving far away from  $\text{PU}_m$  after the first velocity change in order to differentiate from the first situation.  $\varepsilon_b \geq 0$  is used to include all the situations that are not calculated by  $\phi + (T_p^{\text{out}} - \phi) p_b e^{-\lambda(T_p^{\text{out}} - \phi)}$ . According to (2), (24) and (25), the spectrum availability  $A_n^m(T_c)$  for node  $n$  is derived as

$$A_n^m(T_c) = \left( \frac{1}{\lambda T_p^{\text{out}}} + \varepsilon_b + e^{-\lambda T_p} \left( \frac{1}{2} p_b \lambda T_p^{\text{out}} - \frac{1}{\lambda T_p^{\text{out}}} - \varepsilon_b \right) \right) \left( e^{-\mu_p t_0} - e^{-\mu_p (t_0 + T_p^{\text{out}})} \right) + \varepsilon_{\text{in}}. \quad (26)$$

When  $T_p^{\text{out}} \geq T_c$  is satisfied, the spectrum availability is mainly determined by the working state of  $\text{PU}_m$ . Therefore, the spectrum availability  $A_n^m(T_c)$  for node  $n$  is derived as

$$A_n^m(T_c) = \int_{t_0}^{t_0 + T_c} f_{\text{OFF}}(t) dt + \varepsilon_c = e^{-\mu_p t_0} - e^{-\mu_p (t_0 + T_c)} + \varepsilon_c, \quad (27)$$

where  $\varepsilon_c$  denotes all the other spectrum availability situations.

### 3.2 Prediction of Interference Constrains for Cognitive Nodes

The instantaneous interference constrain between two different cognitive nodes is determined by the relative positions in the mobile CR network denoted by (6). The prediction of interference constrain principally investigates whether there is interference



constrain  $\chi_i^j(T_c)$  between cognitive nodes  $i$  and  $j$  from  $t_0$  to  $t_0+T_c$  while there is no interference constrain at  $t_0$ . Those nodes, which have interference constrain at  $t_0$ , are not included. It is due to that the interference constrain of these nodes can be obtained by spectrum sensing technology.

Similar to the analysis method of the prediction for the spectrum availability, let one node predict a continuous time period  $T_p'$  that no interference constrain between the two nodes ( $i, j$ ) will last from  $t_0$  to  $t_0+T_p'$ . In this case, the calculation of no interference constrain from  $t_0$  to  $t_0+T_p'$  is divided into two parts:  $L'_1(T_p') + L'_2(T_p')$ .  $L'_1(T_p')$  indicates the velocities (speed or direction) of the two nodes remain unchanged between  $t_0$  and  $t_0+T_p'$ .  $L'_2(T_p')$  indicates the velocities for any of the two nodes (or both of them) changed between  $t_0$  and  $t_0+T_p'$ . According to(3),  $L'_1(T_p')$  is easy to be obtained as

$$L'_1(T_p') = (1 - B(T_p'))^2 = e^{-2\lambda T_p'} \quad (28)$$

The calculation of  $L'_2(T_p')$  is complicated. Thus, we can get the approximate value  $E(l'_2)$  by estimating  $L'_2(T_p')$ .  $E(l'_2)$  is defined as

$$E(l'_2) = \int_0^{T_p'} l'_2(\varphi) f'(\varphi) d\varphi \quad (29)$$

where,  $l'_2(\varphi)$  is a function of  $\varphi$ . In order to get  $l'_2(\varphi)$ , we calculate the total time of no interference constrain between  $i$  and  $j$ :  $T_i'$ . Assume the first change (any of the two nodes) of velocities happens at  $t_0+\varphi$ . The probability of the velocities keeping unchanged from  $t_0+\varphi$  to  $t_0+T_p'$  for the two nodes is  $e^{-2\lambda(T_p'-\varphi)}$  by(3). Thus,  $T_i'$  can be written as

$$T_i' = \varphi + (T_p' - \varphi) p_{\text{away}} e^{-2\lambda(T_p'-\varphi)} + \varepsilon_{\text{away}} \quad (30)$$

$p_{\text{away}}$  is the probability that the two nodes move far away from each other after the first change at  $t_0+\varphi$  in velocity. In fact,  $\varepsilon_{\text{away}} \geq 0$  tries to include all time periods that are not calculated by  $\varphi + (T_p' - \varphi) p_{\text{away}} e^{-2\lambda(T_p'-\varphi)}$ . Therefore, we can get  $l'_2(\varphi)$  as

$$l'_2(\varphi) = \frac{\varphi + (T_p' - \varphi) p_{\text{away}} e^{-\lambda(T_p'-\varphi)}}{T_p'} + \varepsilon_{\text{away}} \quad (31)$$

$f'(\varphi)$  is defined as

$$f'(\varphi) = \lim_{\Delta\varphi \rightarrow 0} \frac{P(\varphi \leq \Psi < T_p') - P(\varphi + \Delta\varphi \leq \Psi < T_p')}{\Delta\varphi} = \lambda e^{-\lambda\varphi} \quad (32)$$

where  $P(\varphi \leq \Psi < T_p')$  is easy to get as

$$P(\varphi \leq \Psi < T_p') = 2(1 - B(T_p')) \cdot (B(T_p') - B(\varphi)) + (B(T_p') - B(\varphi))^2 = e^{-2\lambda\varphi} - e^{-2\lambda T_p'} \quad (33)$$

Thus, we have  $E(l'_2)$  according to(29),(31)and(32)

$$E(l'_2) = \frac{1}{2\lambda T_p'} + \varepsilon_{\text{away}} + e^{-2\lambda T_p'} \left( p_{\text{away}} \lambda T_p' - \frac{1}{2\lambda T_p'} - \varepsilon_{\text{away}} - 1 \right) \quad (34)$$

When  $T_p' < T_c$  is satisfied, any (or both) of nodes  $i$  and  $j$  should change its (their) velocity

(speed or direction) resulting in the two nodes moving far away from each other before  $t_0 + T_p'$  if there is no interference constrain between them. Accordingly, the appearance probability of interference constrains for nodes  $i$  and  $j$  can be derived as

$$\chi_i^j(T_c) \approx 1 - E(l'_2) = 1 - \frac{1}{2\lambda T_p'} - \varepsilon_{\text{away}} - e^{-2\lambda T_p'} \left( p_{\text{away}} \lambda T_p' - \frac{1}{2\lambda T_p'} - \varepsilon_{\text{away}} - 1 \right). \quad (35)$$

When  $T_p' \geq T_c$  is satisfied, the interference constrain  $\chi_i^j(T_c)$  for nodes  $i$  and  $j$  is derived as

$$\chi_i^j(T_c) \approx 1 - L'_1(T_c) - E(l'_2) = 1 - \frac{1}{2\lambda T_c} - \varepsilon_{\text{away}} - e^{-2\lambda T_c} \left( p_{\text{away}} \lambda T_c - \frac{1}{2\lambda T_c} - \varepsilon_{\text{away}} \right). \quad (36)$$

$p_{\text{away}}$  represents the probability that the two nodes move away from each other after the first change at  $t_0 + \varphi$  in velocity, which makes no interference constrain between them during  $T_c$ .

#### 4. Proposed Prediction-based Spectrum Allocation Algorithms

In this section, two novel prediction-based spectrum allocation algorithms, PFA and PGA, are proposed based on the analysis above.

The main steps of PFA are as follows.

Step1: Initialization. The initial coordinates of the cognitive nodes and the initial states of the PUs are randomly generated in the simulation area. The movements of the cognitive nodes are based on the random walk-based mobility model and the behaviors of PUs follow an exponential on/off traffic model according to (1) and (2). Suppose the probability thresholds of spectrum availability and interference constrains are respective  $\alpha$ ,  $\beta$ , which will be discussed later, and  $v_{\text{max}}$  is the maximum of the velocity for one cognitive node. Additionally, set  $T_c$ ,  $\varepsilon_{\text{away}}$ ,  $p_{\text{away}}$ ,  $\lambda$  and  $\mu_p$ .

Step2: Predict the working states of the PUs based on autoregressive moving average (ARMA) model, which is easy to implement with less computationally expensive [28][29][30]. The ARMA model of order  $(p, q)$  is defined as

$$X_t = \sum_{i=1}^p a_i X_{t-i} + \sum_{j=1}^q \theta_j \xi_{t-j} + \xi_t \quad (37)$$

It is important to choose the order  $(p, q)$  of the model. In this paper,  $p$  and  $q$  are decided by AIC rule, which considers the fitting degree of data. In other words, ARMA  $(p, q)$  should achieve AIC minimum.

Step3: Predict available spectrums of all cognitive nodes. The available spectrum prediction mechanism for a given node  $n$  is shown in **Table 1**. Three situations are considered according to the different value of  $D_{\text{PU}_m, \text{SU}_n}(t_0)$ . When  $D_{\text{PU}_m, \text{SU}_n}(t_0) \geq R + r + v_{\text{max}} \cdot T_c$  is satisfied, spectrum  $m$  is available for node  $n$ . The other two situations have been discussed in section 3.1. Here, the corresponding prediction is done by the relationship between the prediction probability and the decision threshold  $\alpha$ .

Step4: Predict interference constrains of cognitive nodes as shown in **Table 2**. Firstly, calculate the probability of interference constrains for any two different cognitive nodes by (35) when  $T_p' < T_c$  is satisfied and by (36) when  $T_p' \geq T_c$  is satisfied. Secondly, we assume that the interference constrain of two nodes exists when the probability of interference constrain is bigger than  $\beta$ . Otherwise, the interference constrain does not exist.

**Table 1.** Prediction mechanism of available spectrums for cognitive node  $n$ .

<b>Prediction steps of available spectrums</b>
if $D_{P_{Um},S_{Un}}(t_0) \geq R + r + v_{\max} \cdot T_c$ Spectrum $m$ is available for node $n$ . elseif $R + r \leq D_{P_{Um},S_{Un}}(t_0) < R + r + v_{\max} \cdot T_c$ if $T_p < T_c$ Calculate $A_n^m(T_c)$ by (22). else Calculate $A_n^m(T_c)$ by (23). end if $A_n^m(T_c) > \alpha$ Spectrum $m$ is available for node $n$ . end elseif $D_{P_{Um},S_{Un}}(t_0) < R + r$ if $T_p^{\text{out}} < T_c$ Calculate $A_n^m(T_c)$ by (26). else Calculate $A_n^m(T_c)$ by (27). end if $A_n^m(T_c) > \alpha$ Spectrum $m$ is available for node $n$ . end end end

**Table 2.** Prediction mechanism of interference constrain for cognitive node  $i$  and  $j$ .

<b>Prediction steps of interference constrain</b>
if $T_p^i < T_c$ Calculate $\chi_i^j(T_c)$ by (35). else Calculate $\chi_i^j(T_c)$ by (36). end if $\chi_i^j(T_c) > \beta$ Interference constrain exist. else Interference constrain does not exist. end

Step5: All cognitive nodes exchange their link degrees and spectrum degrees. The edges are oriented from a higher spectrum degree to a lower one. When the number of spectrums for two nodes is same, the edge is oriented from a high link degree to a lower one. If a node is a sink node, it picks the spectrum that impact on the minimum number of neighbors. Then, all neighbors remove the spectrum from their spectrum availability lists. The spectrum selection performs from sink to source nodes. After a source node performs the process, the system resets and goes to assign the rest spectrums until all the available spectrums have been assigned.

The main differences between FGA and PFA are determined by the prediction of spectrum availability and interference constrains steps.

For simplicity, the main steps of PGA are given as following. Firstly, all cognitive nodes are ranked by the link degrees from low to high for each channel. Then the channel is assigned to the nodes by the link degrees from low to high. If two nodes have the same link degrees, the node with less assigned channels has higher priority to get a channel.

## 5. Simulation Results and Analysis

In this section, we investigate experimental results of our proposed PGA and PFA algorithms. Simulation parameters are shown in **Table 3**. The system utilities of the prediction algorithms and the traditional algorithms (GA and FA) are compared to evaluate the prediction performances. Note that,  $\varepsilon_a = \varepsilon_b = \varepsilon_c = \varepsilon_{in} = \varepsilon_{away}$  is assumed during the simulation, since they are very small positive numbers in order to balance the according equations.

**Table 3.** Simulation parameters

Parameters	Variable
Total test numbers	5000
Simulation area	5km × 5km
Sample data length for primary spectrum prediction	500
$R$	1km
$r$	0.5km
$T_c$	1s and 5s
$\alpha$	0.8
$\beta$	0.5~0.9
$P_a = P_b = P_{away}$	0.5
$\varepsilon_{away}$	0~0.3
$1/\lambda$	5s and 10s
$1/\mu_p$	0s~15s
Maximum speed of cognitive nodes	0m/s~50m/s
Total Number of PUs	5
Number $N$ of cognitive nodes	10 and 15

According to **Fig. 2**, the fitting degree reaches about 87% when the sample data length is 500. The comparison results turn to be negative, since the original data based on ARMA is dealt with difference. In fact, if the on-off behavior of PUs is more cyclic and stochastic, the prediction result is more accurate. The on-off behavior prediction of PUs remains an open problem, which leaves as our future work.

As shown **Fig. 3**, it can be observed that  $\rho_s$  increases with the increasing of idle PUs, when  $v_{max}$  is a constant. When the number of idle PUs is fixed and less than 4.4,  $\rho_s$  increases with the increasing of  $v_{max}$ . When the number of idle PUs is high (more than 4.4),  $\rho_s$  is not only depended on  $v_{max}$ . Obviously, when the number of idle PUs is high (such as 5), almost each node needs to predict the available spectrum list, which increases the prediction uncertainty. In fact, the prediction uncertainty mainly increases the span of small probability events ( $\varepsilon_a, \varepsilon_b, \varepsilon_c, \varepsilon_{in}$ ), which results in the uncertainty of  $A_n^m(T_c)$  according to (22), (23), (26) and (27).

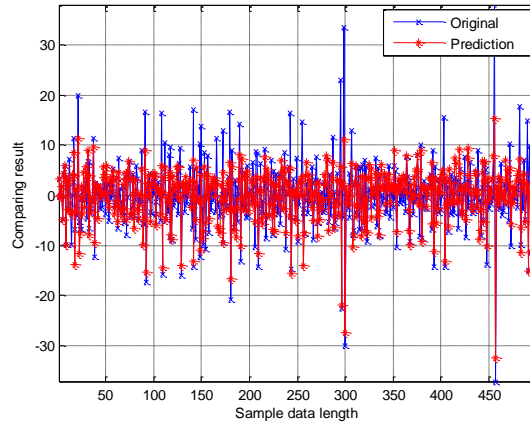


Fig. 2. Comparison between prediction data and original data for the working states of PUs.

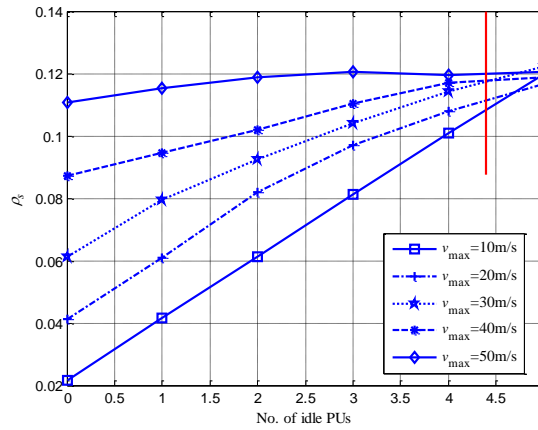


Fig. 3. Available spectrum prediction error rate  $\rho_s$  for cognitive nodes versus No. of idle PUs.

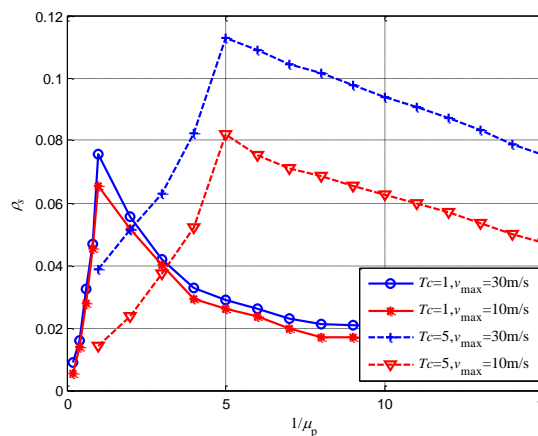
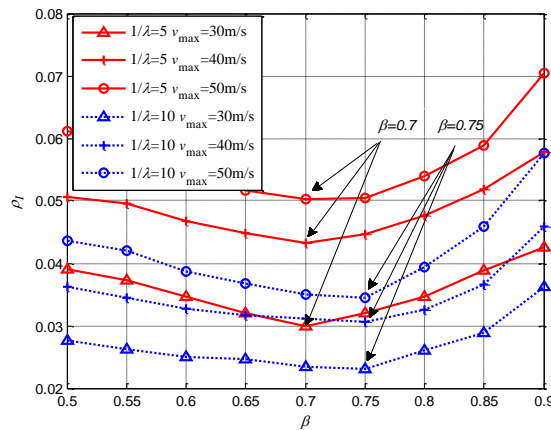


Fig. 4. Available spectrum prediction error rate  $\rho_s$  for cognitive nodes versus  $1/\mu_p$ .

In Fig. 4, the available spectrum prediction performance is studied versus  $1/\mu_p$  and  $T_c$ . As expected, it can be seen from the figure that the prediction with short duration  $T_c$  shows better performance. However, the prediction performance is worse than that of the case  $1/\mu_p = 1$ . In

addition, the worst prediction performance appears at  $1/\mu_p=1$  and  $1/\mu_p=5$  respectively. It is due to the fact that  $\rho_s$  is high under the given threshold when the mean idle time ( $1/\mu_p$ ) of PUs is close to the duration  $T_c$ , which mainly impacts the prediction of spectrum availability for the second situation in section 3.1. Thus, any small deviation of the spectrum availability prediction would lead to a big influence on the decision result, when  $T_c$  is close to the mean idle time of PUs.

**Fig. 5** and **Fig. 6** illustrate the interference constrain prediction error rates under different simulation parameters. In **Fig. 5**, the result was simulated under  $\varepsilon_{\text{away}}=0.1$ ,  $T_c=5$  and  $N=15$ , and  $\beta$  is the variable. When  $1/\lambda$  and  $\beta$  are fixed, it can be seen that  $\rho_l$  degraded continually with the increasing of  $v_{\text{max}}$ . When  $1/\lambda$  and  $v_{\text{max}}$  are fixed, (such as  $1/\lambda=10$ ,  $v_{\text{max}}=30\text{m/s}$ ),  $\rho_l$  has a minimum versus  $\beta$ , which is mainly depended on  $1/\lambda$ . According to (35) and (36), the existence probability of interference constrain is mainly determined by  $1/\lambda$  when  $T_c$ ,  $p_{\text{away}}$  and  $\varepsilon_{\text{away}}$  are given. In fact, the existence of interference constrain is depended on the comparison between the probability and the threshold  $\beta$  based on interference constrain prediction algorithm (**Table 2**). From another point of view,  $1/\lambda$  reflects mean epoch lengths with exponentially distributed. The bigger  $1/\lambda$  is, the more accurate the existence prediction is. The larger  $1/\lambda$  is, the larger  $L'_1(T'_p)$  is according to (28). Thus, false alarm of the interference constrain is decreasing with the threshold  $\beta$  increasing, which is the difference between  $\beta=0.7$  and  $\beta=0.75$ .



**Fig. 5.** Interference constrain prediction error rate  $\rho_l$  for cognitive nodes versus  $\beta$ .

**Fig. 6** shows the impact of  $\varepsilon_{\text{away}}$  on interference constrain error rate prediction  $\rho_l$ . The prediction performance achieves the best  $\rho_l$  when  $\varepsilon_{\text{away}}$  is around 0.15~0.2 with  $v_{\text{max}}$  is a constant. When  $\varepsilon_{\text{away}}$  is relatively larger, the “false alarm” is high. In contrast, when  $\varepsilon_{\text{away}}$  is relatively small, the “false dismissal” would be high. In other words,  $\varepsilon_{\text{away}}$  includes the entire small probability situations by (35) and (36). Thereby,  $\varepsilon_{\text{away}}$  should be selected properly.

According to **Fig. 7**, as expected,  $U_{\text{sum}}$  is almost constant for GA and FA when  $v_{\text{max}}$  increases, since  $U_{\text{sum}}$  takes no consideration of time-varying for spectrum availabilities and interference constrains (regarding to (9)). However,  $U_{\text{sum}}$  decreases gradually for PGA and PFA with the

increasing of  $v_{\max}$ . In fact, the decreasing of available spectrums and the increasing of interference constrains directly lead to the decreasing of  $U_{\text{sum}}$  when  $v_{\max}$  is high, because of the movements of cognitive nodes.

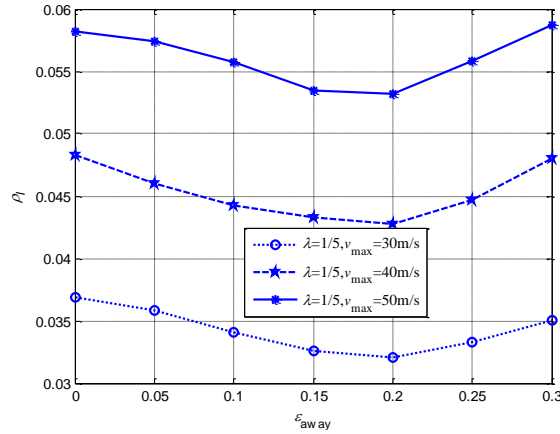


Fig. 6. Interference constrain prediction error rate  $\rho_l$  for cognitive nodes versus  $\epsilon_{\text{away}}$ .

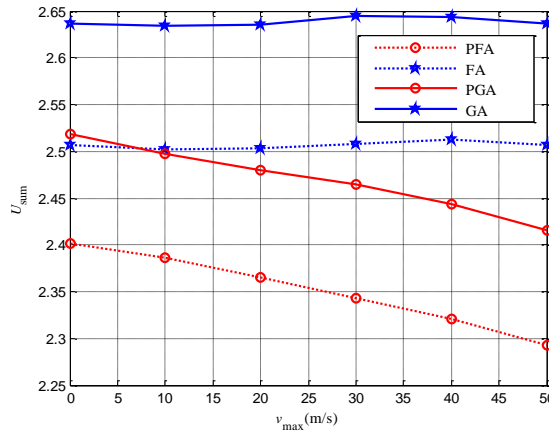


Fig. 7. Comparison of  $U_{\text{sum}}$  versus  $v_{\max}$  for different algorithms.

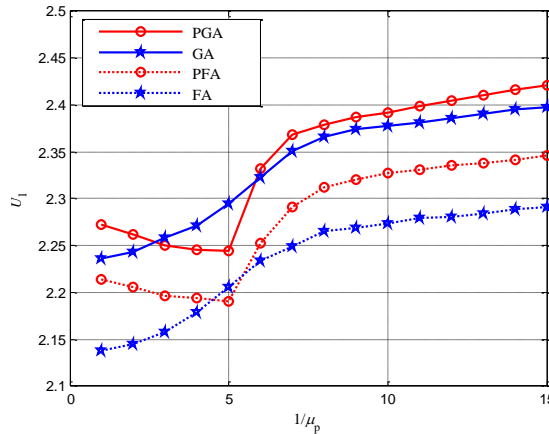


Fig. 8. Comparison of  $U_l$  versus  $1/\mu_p$  for different algorithms.

As shown in Fig. 8, PGA and PFA show good spectrum utilization performance  $U_1$  compared with the traditional GA and FA, when  $1/\mu_p > 6$  is satisfied. It is because the prediction decision of spectrum availability is very strict when  $1/\mu_p$  is close to  $T_c$  ( $1/\mu_p = 5$ ), which has been discussed in Fig.4. The deviation of the prediction result will happen easily according to the prediction mechanism in Table 3. Thus, the poor prediction of the spectrum availability leads to the decreasing of the effective spectrums  $U_1$ . Moreover,  $U_1$  convergent gradually when  $1/\mu_p$  becomes large, since the prediction of spectrum availability is almost correct at this time. Accordingly, there are no more gains with  $1/\mu_p$  increasing.

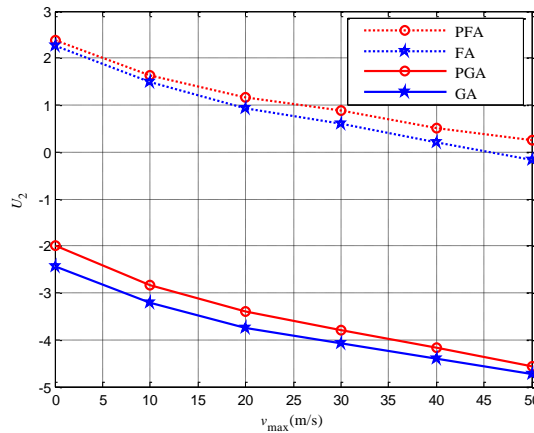


Fig. 9. Comparison of  $U_2$  versus  $v_{max}$  for different algorithms.

As illustrated in Fig. 9,  $U_2$  of our proposed PGA and PFA is higher than the conventional PA and FA respectively. The PFA has the best  $U_2$  among all the four algorithms. When  $v_{max}$  is relatively small, such as “10m/s”, the utility  $U_2$  of PFA is higher than that of FA about 10.6%. When  $v_{max}$  is large enough, such as “40m/s”, the utility  $U_2$  of PFA is higher than that of FA about 143.7%. Actually, PFA shows its prediction profit when  $v_{max}$  is large. However, the utility  $U_2$  of PGA is not so obvious improved compared with GA, when  $v_{max}$  is large relatively, i.e., “40m/s”. The reason is that the goals of GA and PGA are in pursuit of spectrum utilization, not the fairness. In particular, the profits of  $U_2$  for PFA and PGA are from the available spectrum prediction rather than from the interference constrain prediction when  $v_{max} = 0$ .

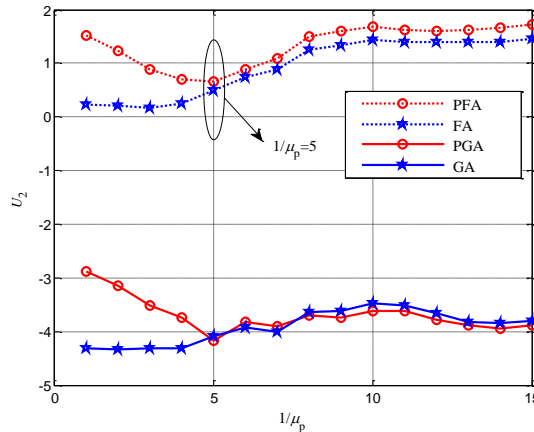


Fig. 10. Comparison of  $U_2$  versus  $1/\mu_p$  for different algorithms.



From **Fig. 10**, it is easy to find that the utility  $U_2$  of PFA is always better than that of FA. The minimum gap between PFA and FA is about 32.2%, when  $1/\mu_p=5$ . It conformers that the prediction performance is worst when  $T_c$  is close to  $1/\mu_p$  again, which we have discussed during **Fig. 4** and **Fig. 8**. The utility  $U_2$  of PGA is better than that of GA when  $1/\mu_p$  is relatively small, due to the prediction gains of PGA. Nevertheless, the utility  $U_2$  of PGA is not better than that of GA when  $1/\mu_p$  is large enough. The reason is that the goal of FGA is in pursuit of maximizing the spectrum utilization instead of the fairness, and the prediction of FGA is accurate when  $1/\mu_p$  is large enough.

## 6. Conclusions

This paper proposed a prediction-based spectrum allocation mechanism in mobile CR network. By the derivation of the probabilities of spectrum availability and interference constrain, we obtained the prediction results of the dynamic available spectrum lists and interference topologies. Simulation results showed that the spectrum utilization of FGA is superior to the other algorithms when the mean idle time of PUs is high, with sacrificing fairness. Nevertheless, the spectrum utilization performance of FGA is worse than that of GA when the prediction decision is not accurate. In addition, PFA gets better fairness performance than the other supervised algorithms. Especially, when the mobile speeds of the cognitive nodes are relatively high, PFA shows its excellent fairness that is more effective and essential to the actual mobile CR network environment.

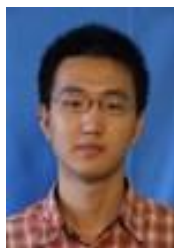
In future we will further analyze the on-off behavior prediction of PUs to obtain a general activity model and fully investigate the impact of  $\varepsilon_{away}$  on prediction performance.

## References

- [1] S. H. Sohn, N. Han, G. B. Zheng, and Jae Moun Kim, "Pilot periodicity based OFDM signal detection method for cognitive radio system," *IEICE Transactions on Communication*, vol. E91-B, no. 5, pp.1644-1647, May, 2008. [Article \(CrossRef Link\)](#)
- [2] N. Han, S. H. Sohn, and J. M. Kim, "A blind OFDM detection and identification method based on cyclostationarity for cognitive radio application," *IEICE Transactions on Communication*, vol. E92-B, no.6, pp.2235-2238, June, 2009. [Article \(CrossRef Link\)](#)
- [3] Zeyang Dai, Jian Liu, Chong gang Wang, and Keping Long, "An adaptive cooperation communication strategy for enhanced opportunistic spectrum access in cognitive radios," *IEEE Communications Letters*, vol. 16, no. 1, pp. 40-43, January, 2012. [Article \(CrossRef Link\)](#)
- [4] M. Thoppian, S. Venkatesan, R. Prakash, and R. Chandrasekaran, "MAC-layer scheduling in cognitive radio based multi-hop wireless networks," in *Proc. of the 2006 International Symposium on World of Wireless, Mobile and Multimedia Networks*, pp. 191-202, June, 2006. [Article \(CrossRef Link\)](#)
- [5] S. Gandham, M. Dawande, and R. Prakash, "Link scheduling in sensor networks: distributed edge coloring revisited," in *Proc. of IEEE INFOCOM*, 4, pp. 2492-2501, March, 2005. [Article \(CrossRef Link\)](#)
- [6] Wei Wang, Xin Liu, "List-coloring based channel allocation for open-spectrum wireless networks," in *Proc. of IEEE 62nd Vehicular Technology Conference*, 1, pp.690-694, September 2005. [Article \(CrossRef Link\)](#)
- [7] Haitao Zheng, Chunyi Peng, "Collaboration and fairness in opportunistic spectrum access," in *Proc. of IEEE International Conference on Communications*, pp.3132-3136, May, 2005. [Article \(CrossRef Link\)](#)

- [8] C. L. Liao, J. Chen, and Y. X. Tang, "Parallel algorithm of spectrum allocation in cognitive radio," *Journal of Electronics & Information Technology*, vol. 29, no. 7, pp. 1608-1611, July, 2007. [Article \(CrossRef Link\)](#)
- [9] Yutao Liu, Mengxiong Jiang, Xuzhi Tan, and Lu Fan, "Maximal independent set based channel allocation algorithm in cognitive radios," in *Proc. of IEEE Youth Conference on Information, Computing and Telecommunication*, pp. 78-81, September, 2009. [Article \(CrossRef Link\)](#)
- [10] Beibei Wang, Zhu Ji, K. J. R. Liu, and Clancy, T.C., "Primary-prioritized Markov approach for dynamic spectrum allocation," *IEEE Transactions on Wireless Communications*, vol. 8, no. 4, pp. 1854-1865, April, 2009. [Article \(CrossRef Link\)](#)
- [11] V. Asghari, Sonia Aissa, "Adaptive rate and power transmission in spectrum-sharing systems," *IEEE Transactions on Wireless Communications*, vol. 9, no. 10, pp. 3272-3280, October, 2010. [Article \(CrossRef Link\)](#)
- [12] E. Jung, Xin Liu, "Opportunistic spectrum access in multiple-primary-user environments under the packet collision constraint," *IEEE/ACM Transactions on Networking*, vol. 19, no. 6, pp. 1-14, April, 2011. [Article \(CrossRef Link\)](#)
- [13] Chengyu Wu, Chen He, Lingge Jiang, and Yunfei Chen, "A novel spectrum handoff scheme with spectrum admission control in cognitive radio networks," in *Proc. of Global Telecommunications Conference (GLOBECOM)*, pp. 1-5, December, 2011. [Article \(CrossRef Link\)](#)
- [14] Xiukui Li, S. A. Zekavat, "Traffic pattern prediction and performance investigation for cognitive radio systems," in *Proc. of Wireless Communications and Networking Conference (WCNC)*, pp. 894-899, March, 2008. [Article \(CrossRef Link\)](#)
- [15] Sixing Yin, Dawei Chen, Qian Zhang, and ShuFang Li, "Prediction-based throughput optimization for dynamic spectrum access," *IEEE Transactions on Vehicular Technology*, vol. 60, no. 3, pp. 1284-1289, March, 2011. [Article \(CrossRef Link\)](#)
- [16] M. Grossglauser, D. N. C. Tse, "Mobility increases the capacity of ad hoc wireless networks," *IEEE/ACM Transactions on Networking*, vol. 10, no. 4, pp. 477-486, August, 2002. [Article \(CrossRef Link\)](#)
- [17] A. C. Talay, D. T. Altılar, "United Nodes: Cluster-based routing protocol for mobile cognitive radio networks," in *Proc. of IET Communications*, vol. 5, no. 15, pp. 2097-2105, October, 2011. [Article \(CrossRef Link\)](#)
- [18] Q. S. Guan, F. R. Yu, S. M. Jiang, and Gang Wei, "Prediction-based topology control and routing in cognitive radio mobile ad hoc networks," *IEEE Transactions on Vehicular Technology*, vol. 59, no. 9, pp. 4443-4451, November, 2010. [Article \(CrossRef Link\)](#)
- [19] Hai Jiang, Lifeng Lai, Rongfei Fan, and Poor, H.V., "Optimal selection of channel sensing order in cognitive radio," *IEEE Transactions on Wireless Communication*, vol. 8, no.1, pp. 297-307, January, 2009. [Article \(CrossRef Link\)](#)
- [20] Zhiqiang Li, R. R. Yu, and Minyi Huang, "A distributed consensus-based cooperative spectrum sensing in cognitive radios," *IEEE Transactions on Vehicular Technology*, vol. 59, no. 1, pp. 383-393, January, 2010. [Article \(CrossRef Link\)](#)
- [21] R. W. Thomas, L. A. Dasilva, and A. B. Mackenzie, "Cognitive networks," in *Proc. of the 1st IEEE International Symposium on New Frontiers in Dynamic Spectrum Access Networks*, pp.352-360, November, 2005. [Article \(CrossRef Link\)](#)
- [22] Anthony McGregor, Mark Hall, Perry Lorier, and James Brunskill, "Flow clustering using machine learning techniques," in *Proc. of 5th Int. Workshop on Passive and Active Network Measurement*, pp.205-214, April, 2004. [Article \(CrossRef Link\)](#)
- [23] C. T. Chou, S. N. Sai, H. Kim, and Shin, K.G., "What and how much to gain by spectrum agility," *IEEE Journal on Selected Areas in Communication*, vol. 25, no. 3, pp.576-588, April, 2007. [Article \(CrossRef Link\)](#)
- [24] H. Kim, K. G. Shin, "Efficient discovery of spectrum opportunities with MAC-layer sensing in cognitive radio networks," *IEEE Transactions on Mobile Computing*, vol. 7, no. 5, pp. 533-545, May, 2008. [Article \(CrossRef Link\)](#)
- [25] Shengming Jiang, Dajiang He, and Jianqiang Rao, "A prediction-based link availability estimation for routing metrics in manets," *IEEE/ACM Transactions on Networking*, vol. 13, no. 6, pp.

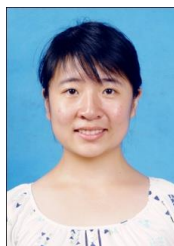
- 1302-1311, December, 2005. [Article \(CrossRef Link\)](#)
- [26] A. B. McDonald, T. F. Znati, "A mobility-based framework for adaptive clustering in wireless ad hoc networks," *IEEE Journal on Selected Areas in Communications*, vol. 17, no. 8, pp. 1466-1487, August, 1999. [Article \(CrossRef Link\)](#)
- [27] Chunyi Peng, Haitao Zheng, and B. Y. Zhao, "Utilization and fairness in spectrum assignment for opportunistic spectrum access," in *Proc. of IEEE International Conference on Communications (ICC)*, pp. 3132-3136, May, 2005. [Article \(CrossRef Link\)](#)
- [28] A. A. Tabassam, M. U. Suleman, "Spectrum estimation and spectrum hole opportunities prediction for cognitive radios using higher-order statistics," *Wireless Advanced*, pp.213-217, June, 2011. [Article \(CrossRef Link\)](#)
- [29] Xiukui Li, Zekavat Reza, and A Seyed, "Cognitive Radio Based Spectrum Sharing: Evaluating Channel Availability via Traffic Pattern Prediction," *IEEE Journal of communications and networks*, vol. 11, no. 2, pp.104-114, April, 2009. [Article \(CrossRef Link\)](#)
- [30] Matthias Wellens, Janne Riihijärvi, and Petri Mähönen, "Empirical time and frequency domain models of spectrum use," *Physical Communication*, vol. 2, no.1 , pp.10-32, March, 2009. [Article \(CrossRef Link\)](#)



**Yao Wang** received the B.S., M.S. degrees in communications engineering from Harbin institute of technology (HIT) in 2007, 2010, respectively. Now, he is currently working toward the Ph.D degree in communication research center, Harbin institute of technology. His major research interests are spectrum resource management and power control in cognitive radio and spread spectrum communication technology.



**Zhongzhao Zhang** received his ph.D. degree in 1997. He is a professor of electronic information engineering school in Harbin institute of technology. His main research interests include data communications, satellite communications, mobile communications, data transmission technology of missile ground station, trunking communication.



**Qiyue Yu** received her B.S., M.S., and Ph.D degrees in communications engineering from Harbin Institute of Technology (HIT), P.R.China, in 2004, 2006, and 2010 respectively. Currently she is a lecturer at the Department of Communications Engineering, HIT. Her research interests include modulation and coding, multiple-access techniques and MIMO for broadband wireless communications.



**Jiamei Chen** received the B.S. and M.S. degrees in Harbin institute of technology. She studied in Purdue University as a visiting scholar from 2011 to 2012. Now, She is working toward the ph.D. degree in communication research center, Harbin institute of technology. Her research interests are 3G and WLAN access resource assignments and cognitive radio.